Comparative study of dielectric liquids for a 2.0kV SiC-MOSFET power module with combined immersion and jet impingement cooling

Johann Renner, Cuong Hoang, Till Huesgen
Electronics Integration Laboratory, Kempten University of Applied Sciences
Kempten, Germany,
johann.renner@hs-kempten.de, cuong.hoang@hs-kempten.de, till.huesgen@hs-kempten.de

Abstract

This paper presents a comparative CFD-study for a novel integration concept for mid-voltage power semiconductor modules. Cooling is primarily achieved through jet impingement on a structured Cu-Inlay from the bottom side and a secondary channel flow directly at the chip top side. This study investigates the thermal performance of three common dielectric coolants (*Shell S5 LV*, *MIVOLT 808*, *MIDEL 7131*) from various application areas. Under realistic boundary conditions (const. current of 50 A), the pumping characteristics are analysed across a coolant temperature range of -20 °C to 60 °C and a junction temperature of 125 °C to 150 °C. The study finds that at a constant flow rate, the thermal resistance ($R_{th,jf}$) varies only marginally between the investigated fluids. However, the viscosity-dependent pressure drop shows significant differences. It is concluded that the thermal management of the power semiconductors remains effective even at low temperatures, provided the coolant remains pumpable within the cooling circuit.

1 Introduction

Conventional packaging technology for medium-power semiconductors (2–10 kV) is based on ceramic substrates as electrical isolators (DBC/AMB) and bond wires for contacting, with the module encapsulated in silicone gel and cooled externally. The main challenge is the trade-off between high electrical insulation (thick ceramic) and good thermal performance (thin ceramic). A promising alternative is immersion cooling with dielectric fluids integrated directly into the module. This method removes solid insulators from the heat flow and enables double-sided cooling of the chips, thus overcoming the thermal limitations. By establishing a significantly shortened thermal path directly from the semiconductor surface to the coolant, this approach facilitates a decrease in thermal resistance and an increase in power density, aligning with the current industry trend toward more compact and lightweight converter systems. Enhanced cooling performance allows for a reduction in the physical footprint of power modules while maintaining or even improving semiconductor reliability through lower junction temperatures. Furthermore, a superior heat dissipation enables a reduction in the required number of parallel chips for a given power rating, which directly translates into lower material costs and more economically competitive module designs.

1.1 Prior Art

Dielectric liquids have long been used for insulation and cooling in power transformers [1], and more recently, for immersion cooling in photovoltaics, data centers, and EV batteries [2] [3]. Immersion-cooled power electronics, such as subsea converters [4] and mid-voltage DC/DC converters for PV systems [5] have also emerged.

Funded by the European Union under GA no. 101172794. Views and opinions expressed are however those of the author(s) only and do not necessarily reflect those of the European Union or CINEA. Neither the European Union nor the granting authority can be held responsible for them.

Our group previously explored jet impingement cooling of PCB-embedded 1.2 kV IGBTs using transformer oil [6]; [7] In the Franco-German *ARCHIVE* project, we developed a 20 kV power module using a ceramic substrate with an integrated liquid cooler, featuring six series-connected 3.3 kV SiC MOSFETs on an AlN substrate integrated cooler [8]. Using *HFE-7500* as the coolant, we achieved excellent thermal performance ($R_{th,jf}$ = 0.47 K/W for a 32 mm² die). Building on the *DiscoPAK* project, which demonstrated a hybrid immersion and jet impingement cooling system for 2 kV SiC MOSFETs [9], this paper further evolves the concept. Prior experimental results using *Shell S5 LV* synthetic oil at 60°C achieved an $R_{th,jf}$ of 0.54 K/W (30 mm² die) at 2.5 l/min per chip.

1.2 Scope of this Paper

While the initial study [9] demonstrated the feasibility of the concept using a single fluid (*Shell S5 LV*) at a fixed temperature of 60 °C, a comprehensive evaluation across the full application range is still missing. Furthermore, as the dielectric insulation capability of an immersion cooling setup for EV applications has already been demonstrated by Chen [10], the present study focuses exclusively on the thermal characterization of the power module. To address the remaining thermal gaps, this analysis expands the investigation to a wider temperature range from -20 °C to 60 °C. Using CFD simulations, the thermal performance of three distinct dielectric fluids is investigated and compared to qualitatively assess their suitability for varying operating conditions and to identify potential thermal limits at extreme temperatures

2 Module Description

Developed within the *DiscoPAK* project, this power module showcases an innovative immersion dielectric cooling concept designed to evaluate the performance boundaries of dielectric fluids in power electronics. The design features a double-sided cooling architecture: primary thermal

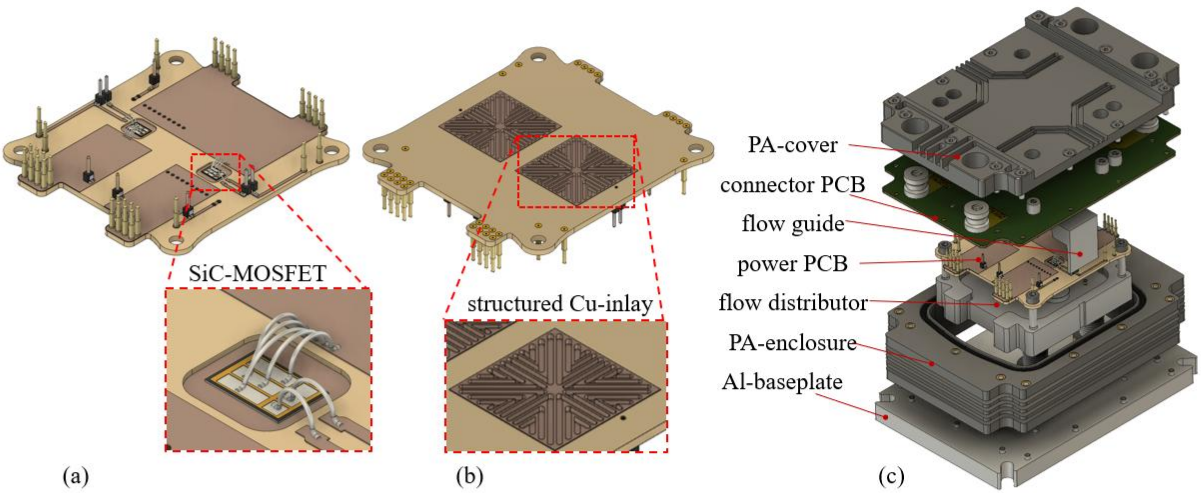

Figure 1: (a) power PCB top view, (b) power PCB bottom view, (c) exploded view

management is achieved via jet impingement targeting the structured backside of the semiconductor, while secondary cooling is provided by fluid flow across the top surface. A key advantage of this approach is the integration of power electronics using mainly standard PCB manufacturing processes, which effectively obviates the need for specialized technical ceramics for electrical insulation.

2.1 Module Structure

The core of the module is the power PCB featuring embedded 1.5 mm copper inlays (**Figure 1**), onto which two 2 kV SiC MOSFETs are silver-sintered. This power PCB is configured as a half-bridge. Electrical interconnection to the connector board is established via spring contacts, while external power connections are facilitated through soldered screw terminals. To ensure environmental sealing, the connector PCB is adhesive bonded to a polyamide cover. The thermal management system consists of a flow distributor below and a flow guide above the power PCB, which collectively direct the coolant flow. The entire assembly is encapsulated in a polyamide housing, using O-rings to seal against the connector PCB at the top and an aluminium baseplate at the bottom. Further design details are provided in [9].

2.2 Flow path

Figure 2 illustrates a cross-sectional view of the module to clarify the coolant path. The dielectric fluid enters through a central inlet in the aluminium baseplate and passes through a flow distributor, which bifurcates the stream and accelerates it into distinct jets. These jets impinge directly onto the structured copper inlays beneath the chips, providing primary cooling at the high-heat-flux zones. Subsequently, the coolant exits through lateral openings in the flow distributor to overflow the top surface of the power PCB (secondary cooling). To enhance heat transfer, a convexly shaped flow guide is positioned above the chips to locally increase the flow velocity.

3 Dielectric Fluids

Driven by the growing research interest in immersion cooling for electric vehicle (EV) batteries and data centers, a wide range of novel dielectric fluids with optimized thermophysical properties has recently emerged. A comprehensive survey (**Table 1**) of common fluids was conducted, from which three promising candidates were selected for further detailed analysis.

Table 1: Comparison of dielectric cooling fluids @20°C

Coolant Type	Coolant	Kin. Viscosity ν mm^2/s	Density ρ kg/l	Therm. Cond. λ W/mK	Spec. heat c_p kJ/kg K	Comments
Water-Based	Water-Glycol 1:1	4,90	1,08	0,40	3,47	Reference cooling fluid
Hydrocarbons	Isovoltine II	10,00	0,88	0,13	1,90	Transformer cooling
	Shell S3 X	9,98	0,78	0,14	2,03	Immersion cooling fluids
	Shell S5 LV	5,90	0,78	0,14	1,91	
	Ampcool AC-110	8,11	0,82	0,14	2,21	
	Electrocool EC-110	7,25	0,82	0,14	2,21	
Ester	Shell EV-Plus TM MIVOLT 808	16,40	0,92	0,13	1,90	Immersion cooling fluid for automotive applications
	Shell MIDEL 7131	74,70	0,97	0,15	1,90	Transformer cooling
Hydrofluorethers	Novec 7100	0,38	1,49	0,07	1,17	to be taken off market due to PFAS discussions
	Novec 7300	0,71	1,62	0,07	1,12	
	Novec 7500	0,77	1,81	0,07	1,06	
	Novec 7700	2,50	0,92	0,07	1,02	
Silicone oil	Dowsil ICL-1000	26,00	0,86	0,18	2,26	Immersion cooling fluid

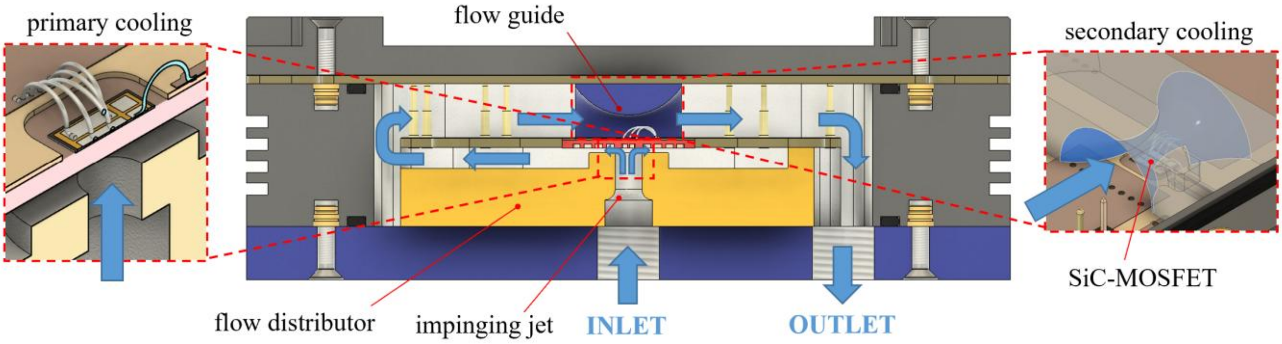

Figure 2: Flow path illustration within power module cross section

Table 2: Selected candidate fluids and their thermophysical properties under -20°C and 60°C

Fluid	Type	Purpose	kin. Viscosity [mm²/s]		Density (kg/m³)		Therm. Conductivity (W/m*K)		Spec. Heat (J/kg*K)	
			-20°C	60°C	-20°C	60°C	-20°C	60°C	-20°C	60°C
S5 LV	synth. Oil & additives	Data Centers	75,0	3,7	822	771	0,148	0,142	1660	2000
MIVOLT 808	synth. Ester	Automotive (EV)	199,0	4,3	945	886	0,138	0,123	1806	2017
MIDEL 7131	synth. Ester	Transformers	1440,0	13,7	1004	939	0,149	0,144	1810	1995
Ref.	Water/Glycol 50%		26,2	1,5	1094	1048	0,366	0,417	3030	3520

For temperatures above 20 °C, most organic coolants typically exhibit thermophysical properties within the same order of magnitude, with the notable exception of viscosity, which varies significantly across different products. Among the evaluated fluids, hydrofluoroethers (HFEs) possess by far the lowest viscosity, theoretically making them ideal candidates for cooling applications. However, these fluids are excluded from further consideration due to the ongoing regulatory scrutiny surrounding per- and polyfluoroalkyl substances (PFAS). It is anticipated that these substances will face restricted availability or complete phase-outs in the near future. The fluids *Shell S5 LV*, *MIVOLT 808* and *MIDEL 7131* were selected as they represent common coolants from various application fields, including data center, EV, and transformer cooling. *Shell S5 LV* represents a data enter coolant with very low viscosity and excellent temperature stability, but also with a very low flash point of 150 °C which makes unsuitable for many applications, such as EV. *MIVOLT 808* represents a coolant specifically developed for the automotive sector. It has a slightly higher viscosity, a flash point of 194 °C and a very wide operating temperature range. *MIDEL 7131* represents a widely known immersion coolant for transformer cooling with the highest flash point of the fluids examined here, at 275°C. However, it also has by far the highest viscosity of the fluids examined. The relationship between increasing viscosity and the associated increase in flash point has already been reported in [10].

Consequently, the selected candidate fluids offer high relevance for the comparative study. However, these fluids exhibit significant differences in the temperature dependence of their viscosity (see **Table 2**). While Shell *S5 LV* maintains a very low viscosity across a wide range, *MIDEL 7131* shows a drastic, exponential increase in viscosity at lower temperatures. Accurately capturing these characteristics in CFD simulations is crucial, particularly for assessing the cold-start behavior of the cooling system. In contrast, the remaining thermophysical properties hardly change within the considered temperature range.

4 Methods

The methods used in this paper are detailed in this section. Specifically, a CFD simulation model provides the fundamental data for subsequent evaluations, while an experimental setup is implemented to validate the simulation results.

4.1 CFD-Simulation Model

The simulations were conducted using Ansys Fluent across two distinct models (see **Figure 3**). Simulations were performed at typical flow rates of 1, 2, 3, 4, and 5 L/min. For both configurations, the k-ω SST turbulence model and a polyhedral mesh were employed.

4.1.1 Hydraulic Model:

A half-model of the overall system used to simulate the pressure drop (Δp). The domain covers the complete internal fluid volume of the module. Thermal equations are not solved in this model. For the fluids under investigation, physical properties were defined based on the specifications provided in the corresponding data sheets.

4.1.2 Hydrothermal Model:

A half-model of a single chip including the cooling structure, employed to simulate the junction temperature (T_j). This model incorporates all components necessary to accurately represent the heat transfer from the chip to the fluid (**Table 3**).

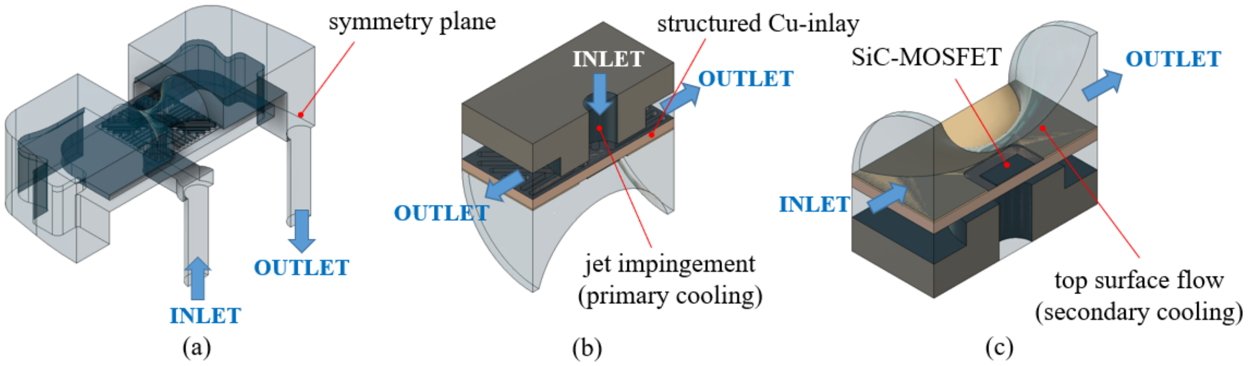

Figure 3: (a) hydraulic model, (b) hydrothermal model bottom view, (c) hydrothermal model top view

Table 3: Relevant component properties for simulation

Component	Property	Value
SiC-Chip	Thermal cond. λ	200 W/(mK)
SiC-Chip	P_{Loss}	144 W
Copper Inlay	Thermal cond. λ	400 W/(mK)
FR4	Thermal cond. λ	0,188 W/(mK)
Sinter Layer	Thermal conductance	$6x10^6$ W/(m²K)

4.2 Experimental Setup

The thermal performance of the power modules is characterized by the junction-to-fluid thermal impedance $Z_{th,jf}$, defined as:

$$Z_{th,jf}(t) = \frac{T_j(t) - T_f}{P_{loss}}$$

where $T_j(t)$ represents the transient junction temperature following a power loss step P_{loss}, and $T_{fluid,in}$ is the coolant inlet temperature. The steady-state value of this impedance is referred to as the thermal resistance $R_{th,jf}$. To determine $Z_{th,jf}$, a constant power loss was applied to the device under test (DUT) using a regulated load current. Upon reaching thermal equilibrium, the load current was disconnected, and the thermal impedance was derived from the cooling transient. The junction temperature was monitored using the body diode voltage of the SiC-MOSFET as a Temperature Sensitive Electrical Parameter (TSEP) at a constant sensing current of 30 mA. Prior to the measurements, a calibration was conducted in a convection oven between 20°C and 110°C, confirming a linear temperature-voltage relationship with a sensitivity of -0.418 K/mV. The experimental setup comprised a Delta SM 18-220 power supply for the load current. The source-drain voltage was recorded for 10sec using a Keysight RIGOL DHO5104 oscilloscope. Rapid disconnection of the load current was achieved via a custom switching stage based on two MOSFETs. To account for initial oscillations (approx. 50 µs) following the turn-off transient, the maximum junction temperature at $t=0$ was determined using the square-root-of-time backward interpolation method. Additionally, a moving average filter was applied to the raw data to minimize noise in the resulting $Z_{th,jf}$ curves. Two fluids (*Shell S5 LV* and *MIVOLT 808*) were tested at a temperature of 60 °C. Five total flow rates were investigated (1, 2, 3, 4, and 5 L/min); accordingly, the flow rate per chip is half of the total volume flow. The experimental setup largely corresponds to the one described in more detail in [9].

5 Results

5.1 Simulation

The results, obtained at flow rates between 1 and 5 L/min, show the junction temperature as a function of the pumping power per chip (see **Figure 4**). With each curve representing a different coolant temperature, the impact of fluid viscosity becomes apparent. Specifically, *Shell S5 LV* shows stable pumping power across the temperature range, whereas *MIDEL 7131* requires significantly higher power at lower temperatures due to its viscosity profile.

5.2 Experimental Validation

Since the power dissipation in the experiments is generated via the current flow through the body diode, it does not match the fixed dissipation of (144 W) used in the simulations. Consequently, the comparison between simulation and measurement in **Figure 5** is based on the thermal resistance ($R_{th,j\text{-}f}$) to ensure a consistent evaluation. The results show that the *Shell S5 LV* simulation closely matches the experimental findings. Interestingly, *MIVOLT 808* slightly outperforms the simulation, yielding improved $R_{th,j\text{-}f}$ values. Due to its higher viscosity, *MIVOLT 808* exhibits a larger pressure drop compared to *Shell S5 LV*, especially at increased flow rates. Overall, the experimental and numerical data align well. Since maintaining lower fluid temperatures during the measurement are currently beyond the capabilities of the laboratory equipment, the remainder of this study relies on the simulation results.

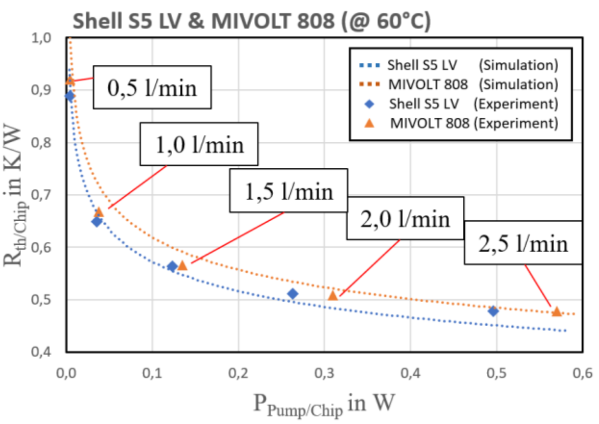

Figure 5: Comparison btw. simulation & measurement

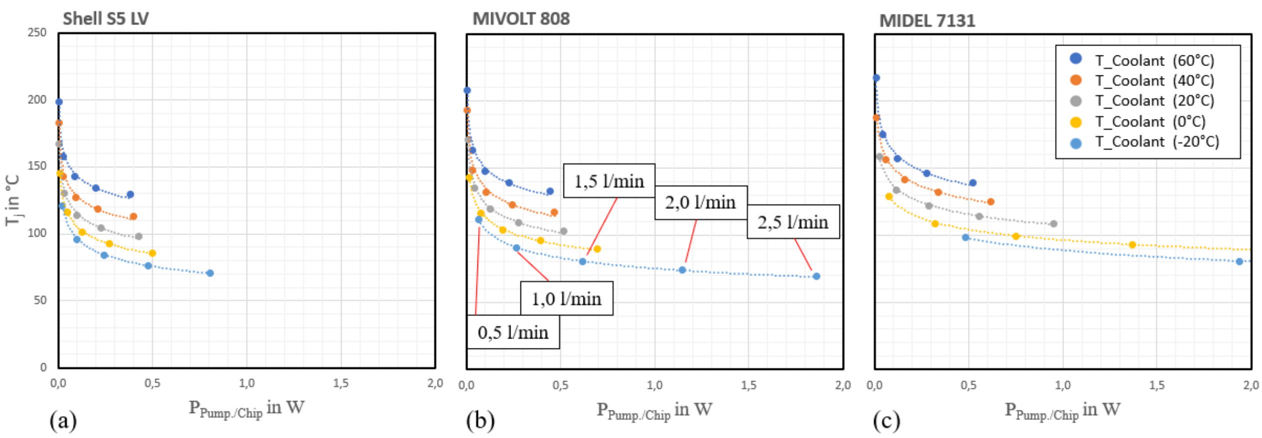

Figure 4: CFD-Simulation results T_j ($P_{Pump/Chip}$) for (a) Shell S5 LV, (b) MIVOLT 808, (c) MIDEL 7131

6 Discussion

While a constant power dissipation of 144 W was used to determine $R_{th,j\text{-}f}$ in the simulation, actual system design is based on the nominal chip current. Since ohmic losses depend on the temperature-dependent $R_{DS(on)}$, the simulation curves must be transformed to reflect a constant current scenario. Using *Shell S5 LV* as an example, we first approximate the simulated data using power functions in the form of:

$$T_{j,CP} = a * P_{hyrd.}{}^{b}$$

This approximation is also shown in **Figure 4** as dashed lines. The maximum deviation of the approximation function from the simulated values is typically only 3%. Here the Index CP stands for constant power and CC for constant current. The graph of *Shell S5 LV* at a coolant temperature of 60°C and a P_{Loss} of 144 W therefore corresponds to:

$$T_{j,CP} = 115{,}8 * P_{hyrd.}{}^{-0{,}092}$$

The power dissipation for the target nominal current is determined by first defining $R_{DS(on)}$ relative to the junction temperature. Using specifications from standard SiC-MOSFET data sheets, this relationship can be modelled for a temperature range from 25 °C to 175 °C using a quadratic polynomial as an approximation function:

$$R_{DS,ON} = \left(2{,}5\text{x}10^{-5} * T_j{}^2 + 0{,}0031 * T_j + 0{,}908\right) * R_{DS,ON@(25°C)}$$

The deviation of this approximation from the data sheet values is typically less than 1%. The power loss is calculated as:

$$P_{Loss,CC} = R_{DS,ON} * I^2$$

The graphs can now be transformed according to:

$$T_{j,CC} = \left(\left(T_{j,CP} - T_{Fluid}\right) * \frac{P_{Loss,CC}}{P_{Loss,CP}}\right) + T_{Fluid}$$

This yields the following graphical representation for a nominal current of I=50 A within the junction temperature range of 125 °C to 150 °C (**Figure 6**):

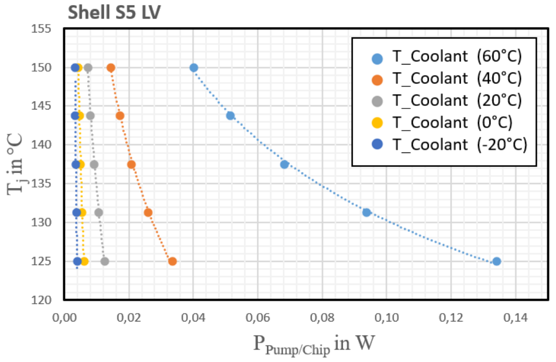

Figure 6: Example of transformed graph for I = 50A

It is noteworthy that the curves become increasingly steep at lower temperatures, which is attributed to the larger ΔT relative to the chip. In this regime, even a minimal change in the flow rate results in a significant reduction of the junction temperature. The described transformation now enables the representation of the required pumping power to maintain a target chip temperature as a function of the coolant temperature (**Figure 7**). The diagram clearly illustrates the impact of the transformation. While the left plot shows the graphs under a constant power dissipation of 118 W, the right plot presents the same scenario under a constant current of 50 A. The dissipation of 118 W corresponds to the chip's power loss at an operating temperature of 125°C and a current of 50 A. Since $R_{DS(on)}$ increases with temperature, more heat must be dissipated, necessitating a higher pumping power to maintain the junction temperature. This is evident from the overall increase in pumping power in the right plot (indicated by red arrow). Notably, for decreasing coolant temperatures, the required pumping power continues to decline despite the increasing viscosity (compare **Table 2**). This can be explained by the fact that the growing temperature gradient between the coolant and the chip becomes the dominant factor; consequently, a very low flow rate is sufficient to maintain the target junction temperature.

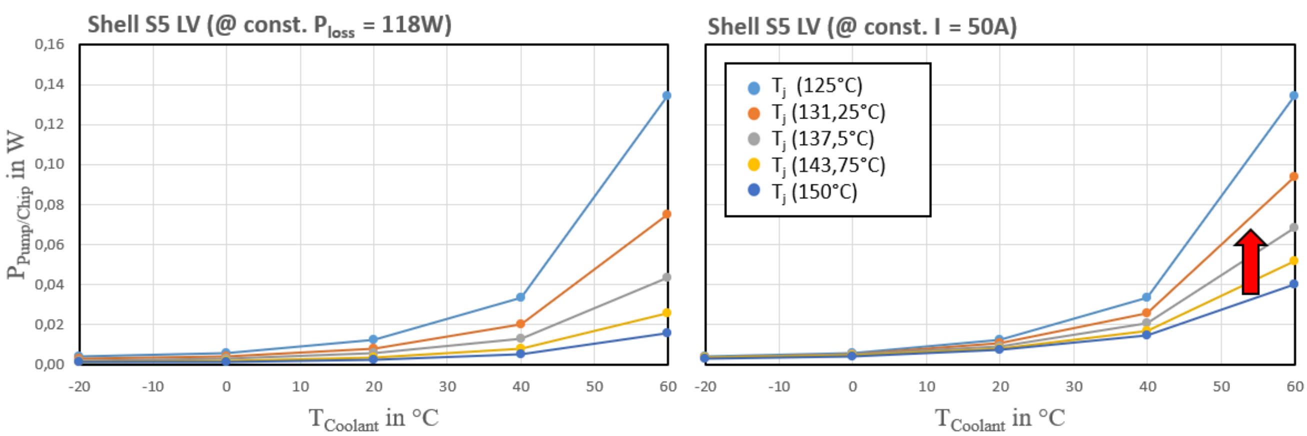

Figure 7: Pumping power per chip as a function of coolant temperature at varying T_j

A comparison of the three fluids (**Figure 8**) at a junction temperature of 125 °C yields the following results:

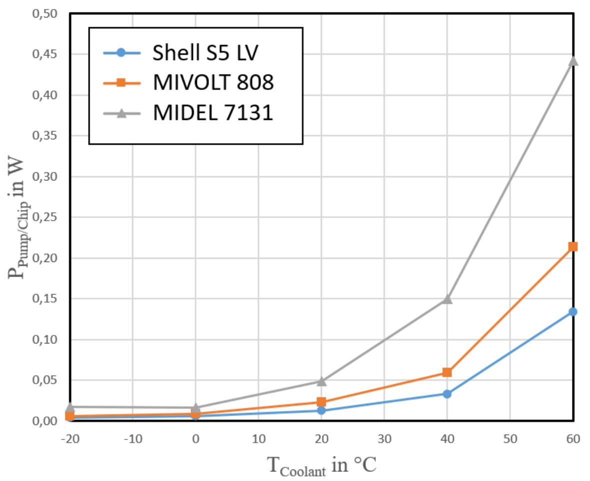

Figure 8: Coolant comparison under T_j = 125 °C

Shell S5 LV requires the lowest pumping power to maintain the target junction temperature due to its low viscosity. In contrast, *MIDEL 7131* exhibits the highest pumping power requirements, which is attributed to it having the highest viscosity among the fluids investigated. Since pumping power is defined as the product of flow rate and pressure drop, both of which are critical parameters for system design and pump selection, these variables must be examined individually. The previously introduced transformation can be applied to the simulation results for both flow rate and pressure drop, assuming that both quantities remain independent of P_{Loss}. **Figure 9** shows the plotted pumping characteristic at various coolant temperatures. Here, the five points along each line represent the five simulated coolant temperatures from 60 °C to -20 °C.

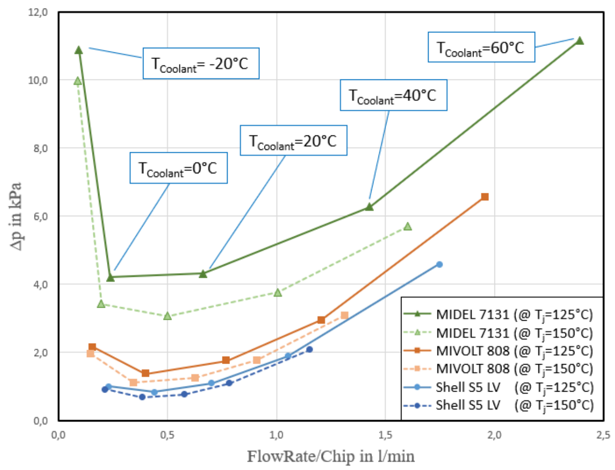

Figure 9: Pumping characteristic of investigated fluids under varying coolant temperature at const. current (50 A) for maintaining a T_j of 125 & 150 °C.

The results indicate that the highest pumping power is required at elevated coolant temperatures (see **Figure 7**). Although the fluid viscosity is lowest at these temperatures, the diminishing temperature gradient between the coolant and the chip represents the most critical thermal constraint. Consequently, maintaining a low junction temperature at high ambient conditions necessitates significantly higher flow rates, where the physical limits are ultimately defined by the module geometry and fluid selection. Conversely, at low temperatures (down to -20 °C), the significantly increased viscosity is counterbalanced by the larger temperature delta between the fluid and the chip. The analysis shows that as long as the fluid remains pumpable at the minimum operating temperature, the junction temperature can be effectively controlled. However, high-viscosity fluids like *MIDEL 7131* exhibit a pressure drop at -20 °C that can exceed the requirements at 60 °C (see **Figure 9** @ T_j=150 °C). For applications with extended requirements (e.g., automotive down to -40 °C), the pressure demand could exceed the capabilities of standard pump systems. In this regard, fluids such as *Shell S5 LV* and *MIVOLT 808* show more favorable characteristics for low-temperature operation. It should be noted that this analysis focused solely on the pressure drop within the power module. In a complete system, the cumulative pressure loss of the entire cooling circuit may be significantly higher.

7 Conclusion & Outlook

This paper investigates the thermal performance of three dielectric coolants (*Shell S5 LV*, *MIVOLT 808*, *MIDEL 7131*) integrated into a previously developed immersion cooling concept. The study encompasses:

- CFD simulations of the junction temperature (T_j) under a constant power loss of 144 W, with coolant temperatures ranging from -20 °C to 60 °C.
- Experimental validation of the simulation models using two selected fluids (*Shell S5 LV*, *MIVOLT 808*).
- A transformation methodology to adapt CFD results from constant power loss to a more realistic application scenario (constant current of I = 50 A).
- An analysis of pumping characteristics for system sizing, comparing the investigated fluids at target junction temperatures of 125 °C and 150 °C.

The results demonstrate that:

- The proposed cooling concept achieves a thermal resistance ($R_{th,j\text{-}f}$) of less than 0.5 K/W at a flow rate of 2.5 l/min per chip.
- At lower coolant temperatures, the increasing temperature gradient between the coolant and the chips becomes the dominant factor, significantly facilitating chip cooling.
- The increased pumping power required due to higher viscosity at low temperatures is negligible for thermal management, provided the dielectric fluid remains pumpable within the cooling circuit.

Future work will involve experimental validation of these CFD results. To this end, the existing test bench will be upgraded with a high-performance chiller to characterize the system performance under extreme temperature conditions.

8 Acknowledgement

The work presented in this paper was conducted within the EU Project “FlagCHIP” (101172794) and utilizes a hardware demonstrator, which was originally developed within ECPE-funded project “DiscoPAK” (2024/PC07). The authors gratefully acknowledge financial support by both funding organizations.

9 Literature

[1] D. K. Mahanta and S. Laskar, "Electrical insulating liquid: A review," *J. Adv. Dielect.*, vol. 07, no. 04, p. 1730001, 2017, doi: 10.1142/S2010135X17300018.

[2] C. Roe *et al.*, "Immersion cooling for lithium-ion batteries – A review," *Journal of Power Sources*, vol. 525, p. 231094, 2022, doi: 10.1016/j.jpowsour.2022.231094.

[3] N. A. Pambudi, A. Sarifudin, R. A. Firdaus, D. K. Ulfa, I. M. Gandidi, and R. Romadhon, "The immersion cooling technology: Current and future development in energy saving," *Alexandria Engineering Journal*, vol. 61, no. 12, pp. 9509–9527, 2022, doi: 10.1016/j.aej.2022.02.059.

[4] A. Petterteig, R. Pittini, M. Hernes, and O. Holt, "Pressure tolerant power IGBTs for subsea applications," in *2009 13th European Conference on Power Electronics and Applications*, 2009, pp. 1–10.

[5] Le Métayer Pierre, "Unidirectional High-Ratio DC-DC Converter for Renewable Energy Sources," INSA Lyon, Dissertation. [Online]. Available: https://theses.insa-lyon.fr/publication/2024ISAL0021/these.pdf

[6] J. Schnur, A. B. Sharma, N. Haag, T. Kuwan, A. Stogel, and T. Huesgen, "Design and Fabrication of PCB Embedded Power Module with Integrated Heat Exchanger for Dielectric Coolant," in *CIPS 2018; 10th International Conference on Integrated Power Electronics Systems*, 2018, pp. 1–6.

[7] A. B. Sharma, J. Schnur, N. Haag, V. Polezhaev, and T. Huesgen, "PCB Embedding using Single-Switch-Pre-Packages as Modular Building Blocks," in *CIPS 2020; 11th International Conference on Integrated Power Electronics Systems*, 2020, pp. 1–6.

[8] A. Al-Hinaai *et al.*, "An Advanced Integrated Cooling Solution for High Voltage and Power Density Modules," in *2023 29th International Workshop on Thermal Investigations of ICs and Systems (THERMINIC)*, Budapest, Hungary, 2023, pp. 1–6.

[9] T. Huesgen, J. Renner, B. Vaidyanathan, and V. Polezhaev, "Dielectric Liquid Cooling of 2.0 kV SiC MOSFET Power Module Using Jet Impingement and Pumped Immersion Flow," in *2025 31st International Workshop on Thermal Investigations of ICs and Systems (THERMINIC)*, Naples, Italy, Sep. 2025 - Sep. 2025, pp. 1–6.

[10] T. Chen *et al.*, "Double-Side Direct Oil-Cooling Automotive Power Module: From Material Compatibility to Thermal Management," *IEEE Trans. on Ind. Applicat.*, pp. 1–12, 2025, doi: 10.1109/TIA.2025.3554465.